研究開発ノート

# A Note for Neoclassical Transport in the Pfirsch-Schlüter Regime of Ultra-Low-Aspect-Ratio Tokamak

FURUKAWA Masaru, WAKATANI Masahiro and SHAING K.C.[1)]
*Graduate School of Energy Science, Kyoto University, Uji 611-0011, Japan*
*[1)] Institute for Fusion Studies, University of Texas, TX, USA*

(Received 29 January 1999/Accepted 15 February 1999)

## Abstract

In the ultra-low-aspect-ratio tokamak, neoclassical viscosity plays a role to enhance the neoclassical transport such as bootstrap current and ion thermal conductivity in the Pfirsch-Schlüter regime. The geometrical factor $\langle(\boldsymbol{n}\cdot\nabla B)^2\rangle$ for calculating the viscosity [K.C. Shaing *et al.*, Phys. Plasmas **3**, 965 (1996)] shows divergent tendency for assumed sequences of numerical MHD equilibria when the aspect ratio is reduced to 1.05, where $\boldsymbol{n}=\boldsymbol{B}/B$ and $\boldsymbol{B}$ is the equilibrium magnetic field.

## Keywords:

ultra-low-aspect-ratio tokamak, neoclassical transport, Pfirsch-Schlüter regime, bootstrap current

A new direction of tokamak research is to study low-aspect-ratio tokamaks (LARTs) or spherical tokamaks (STs). Theoretical studies were started in late 1980's by Peng *et al* [1]. Although several advantages were recognized for the beta limit, transport and divertor, experimental studies were started recently in the small tokamak START (Small Tight Aspect Ratio Tokamak) at Culham Laboratory [2] which showed successful results compared to standard Ohmically heated tokamaks. The success of START stimulated the spherical tokamak research and medium size devices such as MAST (Mega-Amp Spherical Tokamak) [3] and NSTX (National Spherical Torus Experiment) [4] are under construction. Here our concern is in the neoclassical transport in the Pfirsch-Schlüter (P-S) regime of ultra-low-aspect-ratio tokamak (ULART) with $A = R/a \simeq 1$, were $R(a)$ is a major (minor) radius of circular cross-section tokamak.

The neoclassical transport theory including the bootstrap current [5] is a foundation for analyzing confinement properties of tokamak plasmas. It is interesting that the neoclassical ion thermal diffusivity has been observed in the negative shear or enhanced reverse shear configurations [6-8]. The bootstrap current theory also seems consistent with experimental observations [9]. For the ULART it is shown by Shaing *et al.* that the neoclassical viscosity has a divergent tendency for $A \to 1$ in both the banana and P-S regimes [10], which means that the transport behavior in the P-S regime is the same as that in the banana regime. In other words, the bootstrap current or the ion thermal diffusivity is enhanced in the P-S regime and the same expression as in the banana regime is applicable. Thus the bootstrap current is given by

$$J_{\mathrm{b}} = \frac{\langle J_{\|} B\rangle B}{\langle B^2\rangle} = -Ic(\mathrm{d}P/\mathrm{d}\Psi)B/\langle B^2\rangle\,, \tag{1}$$

where $I/R$ is a toroidal magnetic field, $c$ is a velocity of light and $\mathrm{d}P/\mathrm{d}\Psi$ is a radial pressure gradient with respect to the poloidal flux function $\Psi$. The flux surface average is denoted by $\langle\ \cdot\ \rangle$. And the ion thermal diffusivity is given by

$$\chi_{\mathrm{i}} = \sqrt{2}\, N_{\mathrm{i}}\, M_{\mathrm{i}}\, \nu_{\mathrm{i}}\, T_{\mathrm{i}} \left(\frac{Ic}{e}\right)^2 \left\langle \frac{1}{B^2} \right\rangle / |\nabla\Psi|^2\,, \tag{2}$$

where $N_{\mathrm{i}}$ is an ion density, $M_{\mathrm{i}}$ is an ion mass, $\nu_{\mathrm{i}}$ is an

*corresponding author's e-mail: wakatani@energy.kyoto-u.ac.jp*

ion collision frequency, $T_i$ is an ion temperature and the poloidal magnetic field is given by $|\nabla\Psi|$. Equations (1) and (2) are valid for both the banana and P-S regimes of ULART with $A \simeq 1$. These expressions are obtained by including the viscosity-driven contributions to $J_b$ and $\chi_i$ [10]. It is noted that $\nu_a < v_{Ta}[\langle(\boldsymbol{n}\cdot\nabla B)^2\rangle/\langle B^2\rangle]^{1/2}$ is required for applying Eqs. (1) and (2) to the P-S regime, since $A > 1$ in real low aspect ratio tokamaks. Here $\nu_a$ is a collision frequency and $v_{Ta}$ is a thermal velocity of particle species a.

The neoclassical viscosity can be shown as [11]

$$\begin{Bmatrix}\mu_1\\ \mu_2\\ \mu_3\end{Bmatrix} = \frac{8}{3\sqrt{\pi}}\int_0^\infty \mathrm{d}x x^4 e^{-x^2}\begin{Bmatrix}1\\ (x^2-5/2)\\ (x^2-5/2)^2\end{Bmatrix}$$

$$\times\frac{3}{5\nu_T}v_T^2 x^2 F/\langle B^2\rangle\,, \tag{3}$$

in the P-S regime, where the geometrical factor denotes

$$F = \langle(\boldsymbol{n}\cdot\nabla B)^2\rangle\,, \tag{4}$$

$v_T$ is a thermal velocity, $\nu_T = 3\nu_D + \nu_E$, $\nu_D$ is the deflection frequency and $\nu_E$ is the energy exchange frequency. In this formulation $F$ is the important quantity; however, the behavior of $F$ for ULART has not been shown by a numerical code such as NCLASS [12]. Also there is a question whether $F$ will go to infinity or diverge as $A$ approaching unity in realistic equilibria [13]. Thus the purpose of this paper is to show numerical results of the geometrical factor $F$ in realistic ULART equilibria, which were not studied extensively.

The divergent tendency for $A \to 1$ or $\epsilon = 1/A \to 1$ is seen by assuming that the dominant magnetic field is $B = B_0/(1+\epsilon\cos\theta)$ in the Boozer coordinates [14] for calculating Eq. (4) [11],

$$F = (B_0^2/qB_\zeta)^2\frac{\epsilon^2}{2(1-\epsilon^2)^{5/2}(1+\epsilon^2/2)[1+(B_\theta/qB_\zeta)^2]}\,, \tag{5}$$

where $B_\zeta$ ($B_\theta$) is the covariant toroidal (poloidal) component. It is noted that $\langle B^2\rangle = B_0^2/(1+\epsilon^2/2)$.

When the poloidal magnetic field is included through $\Theta = \epsilon/q$ in the model magnetic field $\boldsymbol{B} = [B_0/(1+\epsilon\cos\theta)](\Theta(r)\hat{\theta} + \hat{\zeta})$ for a concentric circular magnetohydrodynamic (MHD) equilibrium,

$$F = \left(\frac{B_0\Theta}{r}\right)^2\frac{\epsilon^2}{2(1-\epsilon^2)^{3/2}}\,, \tag{6}$$

is obtained, and the behavior for $\epsilon \to 1$ does not change. Here $q$ is a safety factor.

Here we will calculate $F = \langle(\boldsymbol{n}\cdot\nabla B)^2\rangle$ for realistic MHD equilibria by changing $A$ with VMEC MHD equilibrium code [15]. In this case we must assume a sequence of MHD equilibria with different aspect ratios. We consider two cases; one is that $q$-profile and $B_t$ at the center of outermost flux surface are fixed, where $B_t$ is a toroidal field. The other is that current profile, $I_p$ and $I_c$ are fixed, where $I_p$ is a total plasma current and $I_c$ is a total current in the center conductor producing the toroidal field $B_t$. Figure 1 shows flux surfaces and constant poloidal angle lines in the VMEC coordinates for MHD equilibria with the lowest aspect ratio $A = 1.05$ for the above two cases. Figure 2 shows the case for the former sequence of circular MHD equilibria and Fig. 3 shows the latter sequence of circular MHD equilibria. Here the minimum of $A$ is 1.05. Both cases show the clear divergent behavior.

The MHD equilibria for Fig. 2 are calculated by keeping the minor radius of circular cross-section $a$ for different $A$ ( or $\epsilon$). The $q$-profile is fixed as $q(s) = q_0(1-s^3) + q_a s^3$, where $s = \Phi/\Phi_a$, $\Phi$ is a toroidal flux function and $\Phi_a$ is $\Phi$ at the plasma surface. The pressure is neglected or a zero beta plasma is assumed. For Fig. 2, a $q$-profile with $q_0 = 1.2$ and $q_a = 3.0$ is kept for different $A$, and $F$ is calculated at the flux surface with $q = 2.5122$. It is noted that the current profile becomes hollow when $A$ is reduced for the fixed $q$-profile. $B_t = 1$ T is also kept constant at the plasma center of circular tokamaks. It seems that numerical results follow Eq. (6) much better than Eq. (5).

For Fig. 3, the current of central conductor $I_c = 15.007$ MA is constant, which corresponds to $B_t = 1$ T at $R = 3$ m. The total plasma current $I_p = 7.7229$ MA is also constant. In this case the current profile is assumed $J(s) = J_0(1-s)$. However, $q_a$ increases significantly, when $A$ is reduced to 1 for the constant minor radius $a$. For $A \simeq 2.4$, $q_a$ less than 1 is taken for obtaining good convergence at $A = 1.05$. The pressure is assumed negligible. It seems again that numerical results follow Eq. (6).

Since the circular flux surfaces are special for ST or LART, we calculate $F$ for $D$-shaped tokamaks with different aspect ratios. Figures 4 and 5 show $F$ as a function of $A$ for $D$-shaped tokamaks with ellipticity $\kappa = 1.64$ and triangularity $\delta = 0.4$. The notation of $\kappa$ or $\delta$ is the same as given by Freidberg [16,17]. In Fig. 4, the $q$-profile with $q_0 = 1.2$ and $q_a = 3.0$ is fixed and $F$ is calculated at the flux surface with $q = 2.5122$. Here $B_t = 1$ T is also kept constant at the plasma center of $D$-shaped tokamaks. In Fig. 5, the total plasma current $I_p = 7.9618$ MA and the current of central conductor $I_c = 15.007$ corresponding to $B_t = 1$ T at $R = 3$ m are

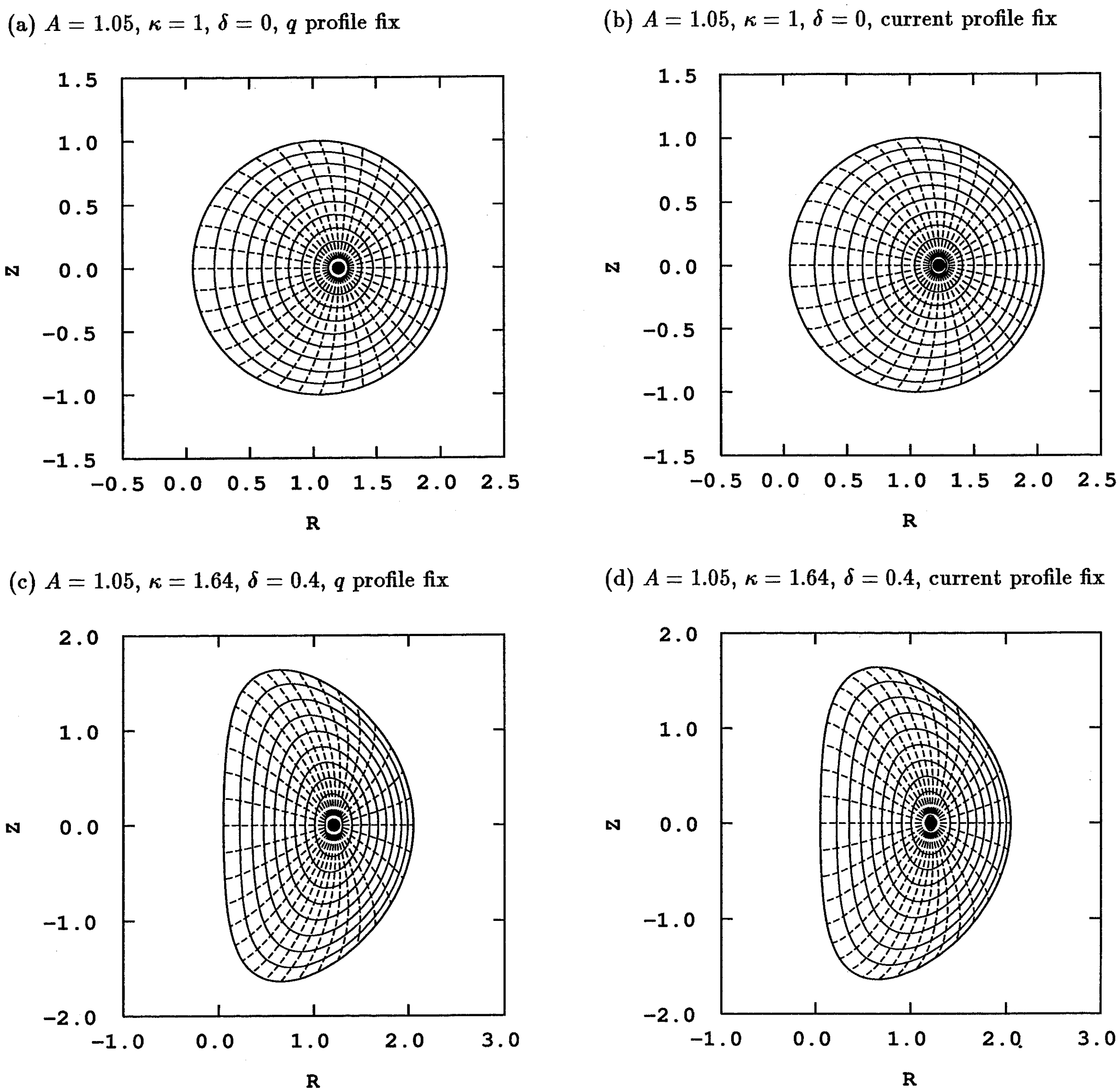


Fig. 1 The lowest aspect ratio equilibria with $A$ = 1.05 are shown, which are included in the following sequences of parameter survey for MHD equilibria. Flux surfaces and constant poloidal angle lines in the VMEC coordinates are plotted; (a) zero-pressure circular tokamak with a given $q$-profile (Fig. 2), (b) zero-pressure circular tokamak with a given current profile (Fig. 3), (c) zero-pressure $D$-shaped tokamak with a given $q$-profile (Fig. 4), and (d) zero-pressure $D$-shaped tokamak with a given current profile (Fig. 5).

fixed for different aspect ratios. It is noted that $F$ also has the divergent tendency in both Figs. 4 and 5.

During the MHD equilibrium calculations of ULART it is found that $q_a$ increases rapidly with $A \to 1$ for the fixed $I_p$ and $I_c$. Katsurai proposed a scaling $q_a \propto (I_c/I_p)/(1-A)^2$ for MHD equilibria of Tokyo University Spherical Torus (TS-3) [18,19]. However, our results give a little slower increase of $q_a$ with $A \to 1$, where $q_a$ and $A$ are taken at the plasma surface in the numerical code. It is found that $q_a \propto (1-A)^{-1.2}$ for the circular cross-section case, and $q_a \propto (1-A)^{-1.4}$ for the $D$-shape case. These scalings may depend on the numerical scheme to solve fixed boundary MHD equilibria in the VMEC.

In summary the expressions (1) and (2) are applicable to the P-S regime of ULART with $A \simeq 1$ under

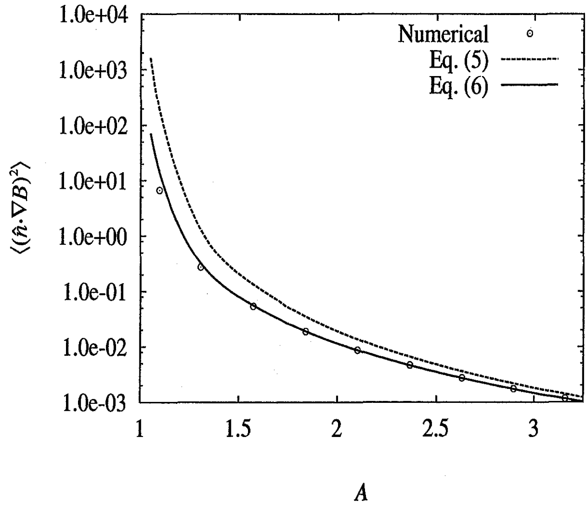


Fig. 2 *F* is plotted as a function of *A* for the fixed *q*-profile and $B_t$ at the plasma center of circular tokamaks. For references Eqs. (5) and (6) are also plotted.

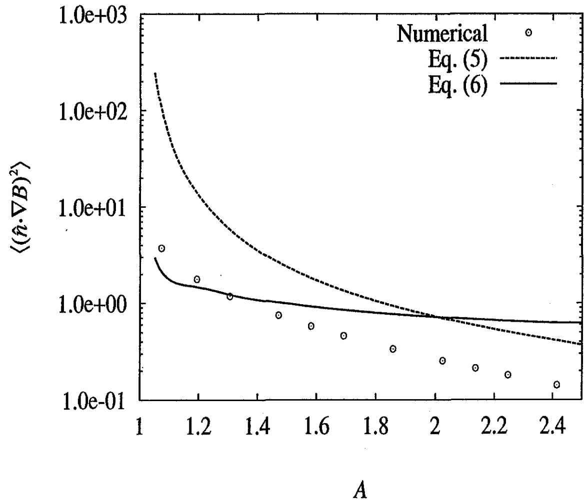


Fig. 3 *F* is plotted as a function of *A* for the fixed current profile, $I_p$ and $I_c$. MHD equilibrium has circular flux surfaces. For references Eqs. (5) and (6) are also plotted.

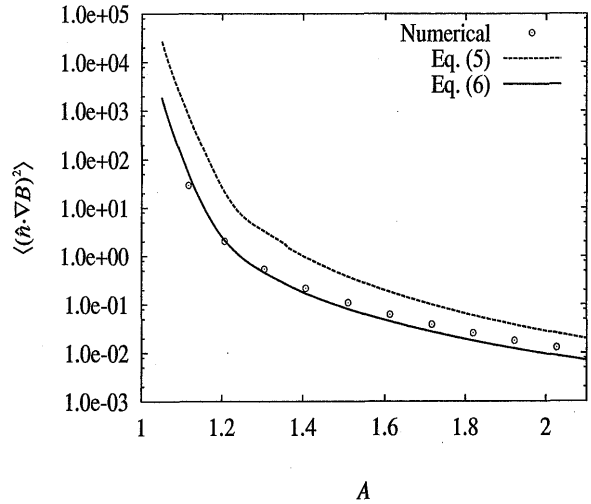


Fig. 4 *F* is plotted as a function of *A* for the fixed *q*-profile and $B_t$ at the plasma center of *D*-shaped tokamaks with $\kappa$ = 1.64 and $\delta$ = 0.4. For references Eqs. (5) and (6) are also plotted, although they are applicable to the circular tokamaks.

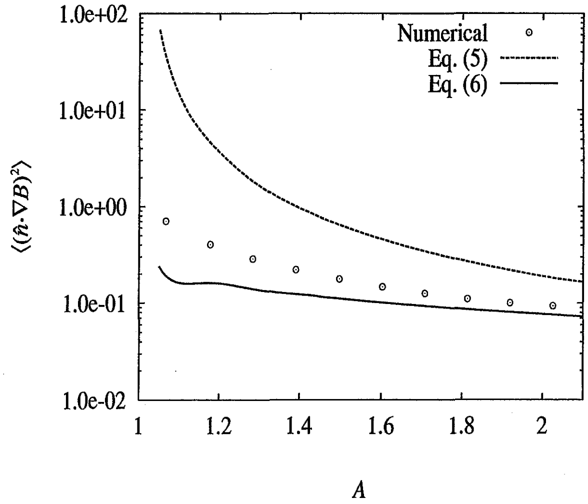


Fig. 5 *F* is plotted as a function of *A* for the fixed current profile, $I_p$ and $I_c$. MHD equilibrium has *D*-shaped flux surfaces with $\kappa$ = 1.64 and $\delta$ = 0.4. For references Eqs. (5) and (6) are also plotted, although they are applicable to circular tokamaks.

reasonable assumptions for the MHD equilibria. However, since $A$ is larger than unity in experimental devices, $\nu_a < v_{Ta}\ [\langle(\boldsymbol{n}\cdot\nabla B)^2\rangle/\langle B^2\rangle]^{1/2}$ is required for applying them to the P-S regime, where $a$ = i for ions and $a$ = e for electrons.

## References


[1] Y-K.M. Peng and D.J. Strickler, Nucl. Fusion **26**, 769 (1986).

[2] A. Sykes, Nucl. Fusion **32**, 694 (1992).

[3] A.C. Darke, M. Cox, J.R. Harbor, J.H. Hay, J.B. Hicks, J.W. Hill, D. Hurford, J.S. McKenzie, A.W. Morris, M.P.S. Nightingale, T.N. Todd, G.M. Voss

and J.R. Watkins, *Proc. 16th Symp. Fusion Engineering* (Urbana-Champaign, 1995) (Institute of Electrical and Electronics Engineers, Piscataway) vol.**2**, p.1456.

[4] J.H. Chrzanowski, H.M. Fan, P.J. Heitzenroeder, M. Ono and J. Robinson, *Proc. 16th Symp. Fusion Engineering* (Urbana-Champaign, 1995) (Institute of Electrical and Electronics Engineers, Piscataway) vol.**2**, p.1430.

[5] F.L. Hinton and R.D. Hazeltine, Rev. Mod. Phys. **48**, 239 (1976).

[6] F.M. Levinton, M.C. Zarnstorff, S.H. Batha, M. Bell, R.E. Bell, R.V. Budny, C. Bush, Z. Chang, E. Fredrickson, A. Janos, J. Manickam, A. Ramsey, S.A. Sabbagh, G.L. Schmidt, E.J. Synakowski and G. Taylor, Phys. Rev. Lett. **75**, 4417 (1995).

[7] E.J. Strait, L.L. Lao, M.E. Mauel, B.W. Rice, T.S. Taylor, K.H. Burrell, M.S. Chu, E.A. Lazarus, T.H. Osborne, S.J. Thompson and A.D. Turnbull, Phys. Rev. Lett. **75**, 4421 (1995).

[8] T. Fujita, S. Ide, H. Shirai, M. Kikuchi, O. Naito, Y. Koide, S. Takeji, H. Kubo and S. Ishida, Phys. Rev. Lett. **78**, 2377 (1997).

[9] M. Kikuchi and M. Azumi, Plasma Phys. Control. Fusion **37**, 1215 (1995).

[10] K.C. Shaing, C.T. Hsu, M. Yokoyama and M. Wakatani, Phys. Plasmas **2**, 349 (1995).

[11] K.C. Shaing, M. Yokoyama, M. Wakatani and C.T. Hsu, Phys. Plasmas **3**, 965 (1996).

[12] W.A. Houlberg, K.C. Shaing, S.P. Hirshman and M.C. Zarnstorff, Phys. Plasmas **4**, 3230 (1997).

[13] Z. Wang, *Proc. 1998 Int. Cong. Plasma Physics* (Prague, 1998), paper To. 46.

[14] A.H. Boozer and G. Kuo-Petravic, Phys. Fluids **24**, 851 (1981).

[15] S.P. Hirshman, W.I. van Rij and P. Merkel, Comput. Phys. Commun. **43**, 143 (1986).

[16] J.P. Freidberg, *Ideal Magnetohydrodynamics* (Plenum Press, New York and London, 1987).

[17] M. Furukawa, Y. Nakamura and M. Wakatani, J. Plasma Fusion Res. **74**, 598 (1998).

[18] Y. Ono, M. Inamoto, T. Okazaki and Y. Ueda, Phys. Plasmas **4**, 1953 (1997).

[19] M. Katsurai, *private communication.*